JOURNAL OF Materials CHEMISTRY

The effect of polymer host on optical absorption spectra for $Er(CF_3SO_3)_3$ in poly(ethylene oxide)

D. Brandell,*[a] M. Klintenberg,[b] A. Aabloo[c] and J. O. Thomas[a]

[a]*Materials Chemistry, Ångström Laboratory, Uppsala University, Box 538, SE-751 21 Uppsala, Sweden. E-mail: brandell@mkem.uu.se*
[b]*Condensed Matter Theory Group, Department of Physics, Uppsala University, Box 534, SE-751 21Uppsala, Sweden and Lawrence Berkeley National Laboratory, University of California, Berkeley, CA 94720, USA*
[c]*Technology Center, Tartu University, Tähe 4 Street, EE51010 Tartu, Estonia*

Received 1st June 2001, Accepted 15th November 2001
First published as an Advance Article on the web 18th January 2002

Erbium triflate, $Er(CF_3SO_3)_3$, salt has been dissolved in poly(ethylene glycol) (PEG400) and analysed at 295 K. The experimental optical absorption spectrum is compared to that calculated using a modified Judd–Ofelt approach. Comparable amorphous polymer–salt systems, $Er(CF_3SO_3)_3$ dissolved in poly(ethylene oxide) (PEO) [EO : Er ratios 100, 50, 28.6 and 25 : 1] have been simulated at 300 K using molecular dynamics (MD) and the different MD-generated rare earth environments have been used to calculate crystal-field parameters. A variety of coordination types are found for the Er^{3+} ions. Agreement between the calculated and experimental spectra is quite satisfactory; discrepancies can be ascribed to inappropriate free-ion parameters and the crystal-field model used.

1. Introduction

Recent years have seen an increasing interest in rare-earth doped polymer systems following innovative discoveries in the chemistry of polymer solutions, and motivated by the wide range of potential applications.[1] Luminescent polymers have typical applications in novel optical displays, detectors, fluorescent lighting, and in a diversity of opto-electronic applications. By comparison with the widely used rare-earth doped glasses and crystals, polymer systems have the striking advantages that they are stable, cheap, ecologically acceptable and easily manufactured.

It is well known that the coordination of the rare-earth ion to the host material, or to a complex of macromolecules, is critical to the optical properties of the material.[2] Understanding of local structure, coordination geometries, *etc.* is therefore necessary for a detailed understanding of the optical properties in these kinds of rare-earth polymer system. In this context, computational methods and different kinds of spectroscopic technique are valuable tools.

Judd–Ofelt theory[3,4] has proven a useful tool for deriving the 4f–4f oscillator strengths for the rare-earth ions. A simulated spectrum can be constructed by accumulating oscillator strengths for a number of MD-generated snapshot structures. By adding the contributions from all rare-earth ions in the MD simulation box from a sequence of such snapshots, we can construct a complete spectrum and compare it to experiment. A slightly modified Judd–Ofelt theory has been used, facilitating the calculation of the individual Stark level transition probabilities.

In this work, we have studied different concentrations of $Er(CF_3SO_3)_3$ in poly(ethylene oxide) ("PEO" = $-(CH_2-CH_2-O)_n-$). This can be treated as a model for more complex systems involving a lower degree of coordination of the rare earth ion to the polymer, which are more useful in optical devices. The reason for using the somewhat bulky triflate anion, $CF_3SO_3^-$, is that mono-atomic anions tend to form clusters in polymer hosts[5] with no "plasticizing" effect on the polymer, and there is experimental evidence of complete dissolution of lanthanide triflate salts in PEO.[6]

MD simulations were performed for Er : EO ratios 1 : 100 to 1 : 25. These concentrations are generally too high for potentially interesting rare-earth polymer systems, but interesting as model systems for analysing structural properties. The absorption spectra were obtained for $Er(CF_3SO_3)_3$ dissolved in liquid poly(ethylene glycol) (PEG400); a shorter form of PEO. Low molecular-weight host polymers such as PEG400 can be used as model systems without influencing the optical properties; however, they minimise the light scattering from the micro-crystalline regions in higher molecular-weight polymers such as PEO. The number of monomers (8–9) is likely to reproduce the symmetry and conformation properties of high molecular weight polymer analogues used in the simulations and in most technological applications.[7]

2. Molecular dynamics (MD) simulation

MD simulations were performed using a simulation box containing a 200-monomer chain of PEO and $Er(CF_3SO_3)_3$ with Er : EO ratios 1 : 100, 1 : 50, 1 : 28.6 and 1 : 20 (corresponding to 3.33, 5.94, 8.93 and 9.75 wt% rare earth, respectively). The salt ions were distributed randomly in the box containing the amorphous polymer. The intramolecular potential model used for PEO has been described in reference 8 and the triflate potentials in reference 9. The non-bonded interactions have been parameterized using the standard ion-pair Born–Mayer–Huggins potential form:

$$V(r) = \sum_{(i \neq j)} \frac{q_i q_j}{4\pi\varepsilon_0 |r_{ij}|} + A \cdot \exp\left(-\frac{|r_{ij}|}{B}\right) - \frac{C}{r_{ij}^6} \qquad (1)$$

The Er–PEO interaction potentials are described in reference 5 and the PEO–triflate potentials calculated using universal force field (UFF),[10] while the Er–triflate interaction potentials were generated from fitting the constants A, B and C in the above

DOI: 10.1039/b104805h

Table 1 Born–Mayer–Huggins potential parameters [see eqn. (1)]

Atom pair	A/kcal mol^{-1}	B/Å	C/kcal Å^6 mol^{-1}
O···O	58298.9	0.24849	192.1
O···C	42123.0	0.27418	352.8
O···H	19497.1	0.24450	98.8
O···S	118400.1	0.26790	631.1
O···F	71407.7	0.32800	153.1
C···S	85818.8	0.29560	1156.9
C···C	31615.1	0.30251	647.8
C···H	14953.8	0.27151	181.5
C···F	50669.8	0.26260	280.2
S···S	240523.5	0.28890	2072.9
S···F	144805.3	0.25660	502.8
S···H	39793.5	0.26360	323.1
F···F	88221.2	0.22790	122.1
F···H	23213.2	0.23410	78.2
H···H	7161.2	0.24050	50.8
Er···Er	21441.3	0.21333	2846.0
Er···S	61299.4	0.27368	2245.1
Er···F	430671.8	0.19999	−322.5
Er···C_{poly}	260359.0	0.25404	0.0
Er···O_{poly}	2353533.7	0.23024	0.0
Er···H	123913.4	0.22651	0.0
Er···O_{trifl}	452509.1	0.04314	−5435.0
Er···C_{trifl}	44592.4	0.28851	1785.4

expression to *ab initio* calculated energy values (adiabatic potential energy surface, APES).[11] The APES was sampled using several conformations of Er^{3+} around a triflate molecule, and the resulting pair potentials are listed in Table 1.

The MD simulations were performed using the program DL_POLY_2.0.[12] The initial polymer configuration was created prior to this work using a pivotal Monte Carlo technique, and the salt ions were inserted randomly into adequate spaces in the simulation box. The simulations were performed at 300 K and 1 bar pressure. Equilibration was achieved using a Nose-Hoover NVT thermostat, and the NPT thermostat was used thereafter (for 1 ns). The time-step used in the simulation (Δt) was 0.5 fs. An Ewald summation routine was used in calculating the electrostatic potentials, with a conversion parameter α of 0.28461 Å^{-1} and with maximum k-vector indices $k_x = 7$, $k_y = 6$ and $k_z = 6$. The short-range cut-off was 10 Å and the Verlet sphere used in the Verlet neighbour list construction had a radius of 1.2 Å.

3. Calculation of spectra

300 snapshots taken every 1000 time-step of the final NPT phase of the MD simulation were used to generate the crystal-field parameters for each of the different Er^{3+} ions. These parameters, essential for the calculation of energy levels and intensities, were calculated within the electrostatic multipole-expansion model:[13]

$$A_q^{(k)} = \sum_j q_j r_j'^{-k-1} C_q^{(k)}(\hat{r}_j) \tag{2}$$

Here only the monopole term has been considered.

To calculate the Stark energy levels for the Er^{3+} ions, a perturbation approach was used to raise the degeneracy in the 364-fold degenerated $4f^{11}$ configuration. The Hamiltonian used was:

$$H = H_0 + H_{EL} + H_{SO} + H_{CIL} + H_{CINL} + H_{CF} \tag{3}$$

where H_0 is a spherically symmetric interaction and is therefore omitted (it only shifts the whole configuration), *i.e.* the energy corresponding to the degenerate configuration is set to zero; H_{EL} is the coulomb interaction; H_{SO} is the spin–orbit interaction; and H_{CF} is the crystal-field interaction dependent on the Er^{3+} ion environment. H_{CIL} and H_{CINL} represent the linear and non-linear configuration interactions,[14,15] respectively.

Table 2 Free-ion parameters

Parameter	Value/cm^{-1}
F^2	98 679
F^4	70 767
F^6	51 623
ζ	2361.2
α	18.852
β	−692.11
γ	1470.8
T^2	0
T^3	75
T^4	98
T^6	−160
T^7	235
T^8	0

Table 3 Shielding parameters and radial matrix elements

Parameter	Value
σ_2	0.460
σ_4	0.0190
σ_6	−0.0283
$<r^2>$	0.773
$<r^4>$	1.677
$<r^6>$	8.431

The energies and eigenvectors needed for the construction of the spectrum were obtained by diagonalizing the energy matrix. The matrix elements were described in the *SLJM* representation:

$$< \gamma SLJM|H|\gamma' S'L'J'M' > \tag{4}$$

A detailed description of the calculation of the matrix elements and the perturbation calculations can be found in references 16–18 and the parameter values used (from references 13,19) are listed in Tables 2 and 3.

The Judd–Ofelt theory describes induced electric-dipole transitions between J manifolds in the 4f shell of rare earth ions. In this work, transitions between JM_j levels have been considered. The oscillator strength is given by the "Fermi golden rule" expression:

$$P_q = \frac{1}{2}\chi\frac{8\pi^2 m\nu}{h}\left|< i|D_q^{(1)}|f >\right|^2 \frac{e^{-E_i/k_BT}}{\sum_j e^{-E_j/k_BT}} \tag{5}$$

where m is the electron mass, h is Planck's constant, ν is the relevant transition frequency, χ is the Lorentz local-field function, and $D_q^{(1)}$ is the dipole operator. A detailed description of the calculation of $<i|D_q^{(1)}|f>$ can be found in reference 17 where the standard Judd–Ofelt intensity parameters are calculated from the crystal-field parameters.

4. Experimental

The triflate salt, $Er(CF_3SO_3)_3$, was prepared by dissolving 99.9% $Er_2(CO_3)_3$ in aqueous HCF_3SO_3 (trifluoromethanesulfonic acid) until pH ≈ 5 followed by precipitation at ~70 °C. The resulting salt, which had a pink colour, was dried under vacuum at 140 °C, and then dissolved into the liquid polymer host polyethylene glycol (PEG400) with an Er : EO ratio of 1 : 25. The dissolution was complete. An absorption spectrum with resolution 1 nm in the interval 200–800 nm (Fig. 1) was obtained on a Perkin-Elmer Lambda 2 UV/VIS spectrometer.

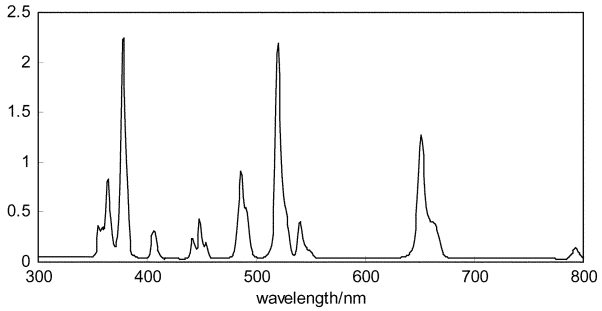

Fig. 1 Experimental optical absorption spectrum for $Er(CF_3SO_3)_3$-$(PEG400)_{25}$.

5. Results and discussion

5.1 Ion-clustering phenomena in the simulations

The fact that the system remains amorphous in the simulations and does not tend to phase-separate at these concentrations is evidenced by several observations:

The content of the simulation boxes after simulation shows no indication of significant clustering. The clusters which form generally consist of one Er^{3+} ion, one or two sections of PEO chain, and a pair of triflate ions. We see in Fig. 2 for the highest salt concentration (Er : EO ratio 25 : 1) that the distances between the Er^{3+} ions observed in the figure indicate only limited formation of larger clusters.

Radial distribution functions show no evidence of short-range interactions between the Er^{3+} ions, as was observed in systems involving the mono-atomic anion Cl^-.[5] This clearly indicates that Er^{3+} ions tend to lie well separated from one other.

Only 25% of the triflate ions coordinate to more than one Er^{3+} ion. If the system tended to crystallise, this figure would have been much higher, with all triflates coordinating to several Er^{3+} ions. This also indicates that there is no rare-earth ion clustering, indicating only very limited risk for concentration-quenching.

5.2 Coordination

The Er^{3+} ions are generally found to have coordination numbers ranging from 7 to 10, with an average value of 9; values which are in good agreement with those observed for rare earth ions occurring in many different systems, suggesting that our MD potentials are reasonably appropriate. The Er^{3+} ion shows a striking tendency to coordinate to polymer or triflate oxygens; only one of the erbium ions in the simulations was found to coordinate to anything else (a triflate fluorine), and then as a part of a larger complex.

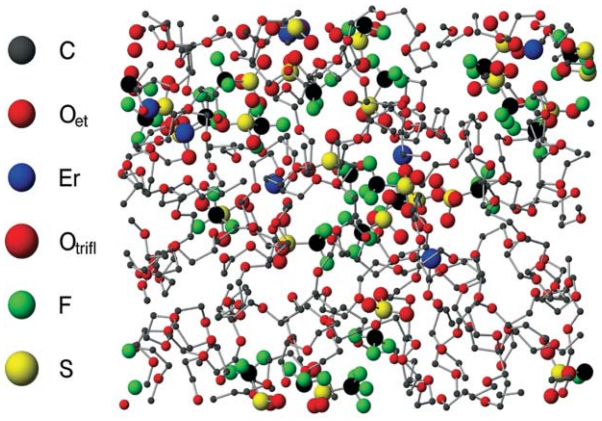

Fig. 2 A snapshot of the MD simulation box for $Er(CF_3SO_3)_3(PEO)_{25}$ containing 200 EO monomers, 8 Er^{3+} ions and 24 triflate ions.

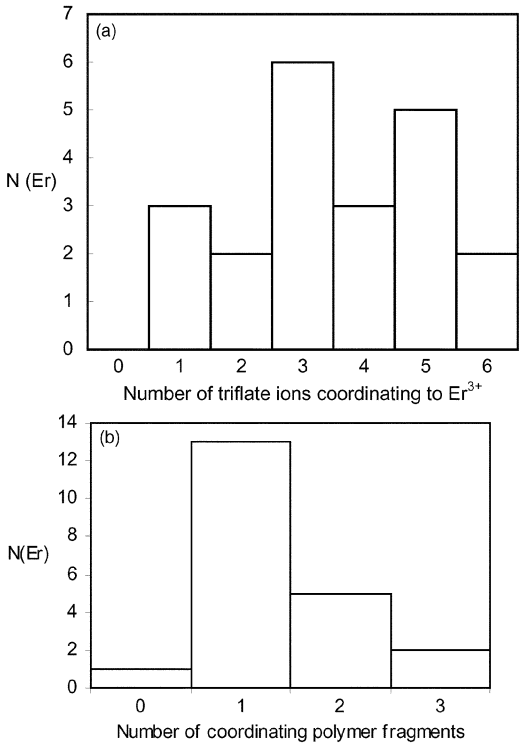

Fig. 3 The distribution of coordination numbers in the simulations for triflate ions to Er^{3+} (a); and the number of polymer-chain segments coordinating to Er^{3+} (b).

However, there is a rich variation in the coordination between the different Er^{3+} ions in the simulation, and the observed coordination numbers to triflate oxygens have a considerable range of distribution (Fig. 3a). Radial distribution functions (Fig. 4) show that the PEO ether oxygens generally coordinate to Er^{3+} at distances 2.5–3.0 Å, while the triflate oxygens coordinate at distances 2.3–2.5 Å. This can be expected since the triflate oxygens carry a somewhat higher partial charge.[8,9] All triflate ions coordinating to Er^{3+} ions did so along only one of the three S–O bonds (Fig. 5). These

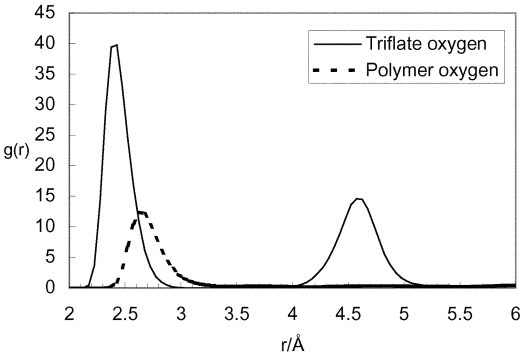

Fig. 4 Er–O radial distribution function for $Er(CF_3SO_3)_3(PEO)_{25}$.

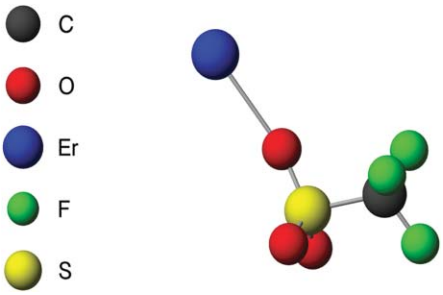

Fig. 5 Typical coordination for $CF_3SO_3^-$ to Er^{3+} in $Er(CF_3SO_3)_3$-$(PEO)_n$.

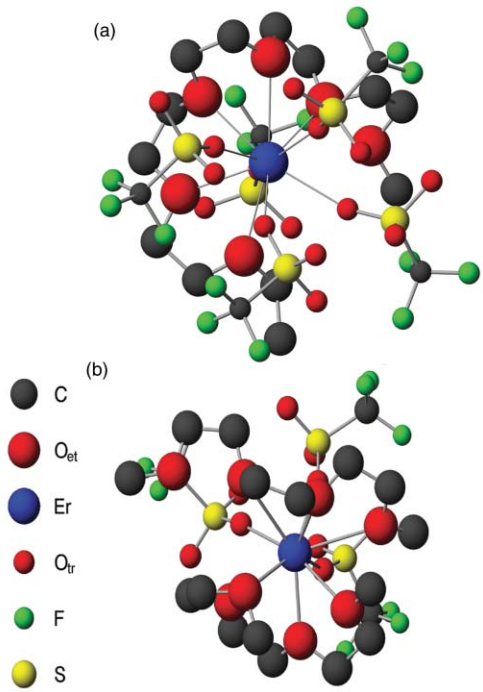

Fig. 6 Er^{3+} coordinating to: (a) one polymer segment of EO and four triflate ions; and (b) two polymer segments and three triflate ions in $Er(CF_3SO_3)_3(PEO)_{25}$.

variations in coordination suggest that the crystal-field parameters should be different for different Er^{3+} ion environments, and thus give different contributions to the spectra.

The polymer also coordinates directly to the rare earth ion in a number of ways (the distribution is shown in Fig. 3b). The most common case, observed for more than 60% of the Er^{3+} ions, is that a successive sequence of PEO ether oxygens wraps itself around the rare earth ion (Fig. 6a). When Er^{3+} ions coordinate to a large number of ether oxygens (>7), two or even three separate sections of PEO chain wrap around the same ion (Fig. 6b). These observations suggest that the highly charged rare earth ions induce rigidity in the "coordinating" polymer backbone.

5.3 The calculated spectrum

The most striking feature of the calculated spectra is the clear similarity between the different concentrations (see Fig. 7). This is not unreasonable since the same types of local environment appear in MD simulations for all concentrations. On summing the crystal-field parameters which influence the rare earth ions over the entire MD box for all snapshots, this result is generally independent of concentration.

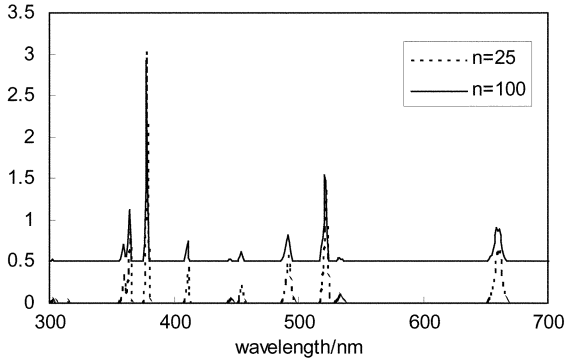

Fig. 7 The calculated optical absorption spectra for $Er(CF_3SO_3)_3(PEO)_{25}$ and $Er(CF_3SO_3)_3(PEO)_{100}$.

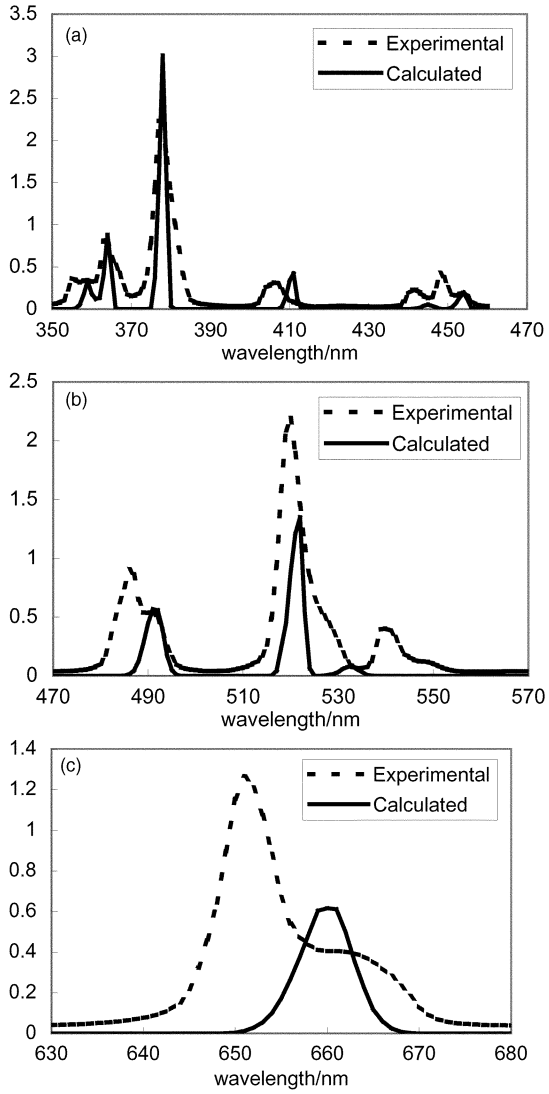

Fig. 8 Comparison between the experimental spectrum for $Er(CF_3SO_3)_3(PEG400)_{25}$ and the calculated spectrum for $Er(CF_3SO_3)_3(PEO)_{25}$.

The calculated spectra have been constructed with the same resolution as the experimental spectrum: 1 nm.

5.4 Comparison with the experimental spectrum

No major differences appear between the calculated and experimental spectra (Fig. 8). The differences that do occur, such as the variation in bandwidth and small shifts of the energy levels, can be traced back to the free-ion parameters used in the matrix construction (Tables 2 and 3), which were all determined for other chemical systems. Re-fitting these parameters to the experimental data obtained here would improve the agreement. However, this has not been done since these parameters are best obtained from low temperature studies. Experimental line-broadening effects can also explain the differences in bandwidth.

What is more striking and unexpected is the similarity between the spectral contributions from different local environments (Fig. 9). Since different local environments generate different crystal-field parameters, some differences in the spectra would be expected; this is the case for Cl^- as anion.[5] Although small differences can be seen, no general trends in the spectral contributions from the different local environments can be discerned. All contributions from different environments differ internally by less than they differ compared to the corresponding experimental peak (Fig. 9e). It would

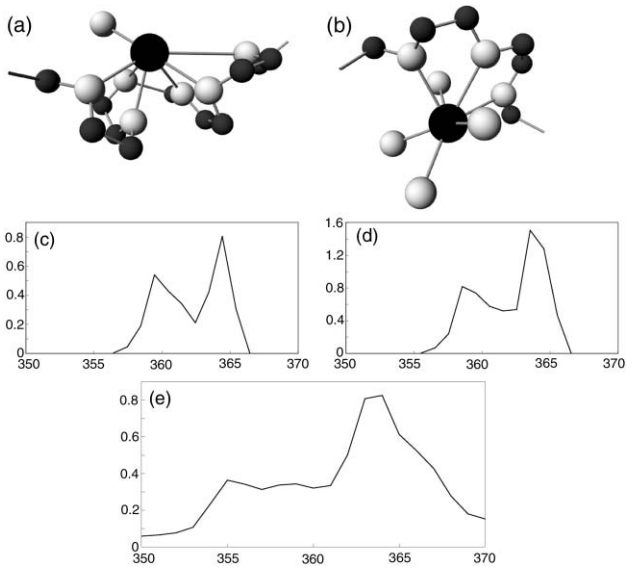

Fig. 9 Two different local environments around Er^{3+}, (a) and (b), and their spectral contributions, (c) and (d), compared to the corresponding experimental peaks (e): $^4I_{15/2} \rightarrow {}^4G_{9/2}$, $^4I_{15/2} \rightarrow {}^2K_{15/2}$ and $^4I_{15/2} \rightarrow {}^4G_{7/2}$ for $Er(CF_3SO_3)_3(PEG400)_{25}$.

therefore not seem meaningful at this stage to attempt to derive information relating to the relative abundance of different local environments on the basis of a fit of theoretical to experimental data, although this is our ultimate goal.

Since the difference in spectral contribution between the different coordination types originates in the crystal-field parameters, it is clear that the crystal-field model must be lacking in sophistication. That the Er^{3+} ions coordinate almost exclusively to oxygen atoms gives some indication of where improvements must be made. The crystal-field model used, which only takes account of the monopole contribution, would not appear to be able to distinguish the different local environments which can arise. A crystal-field model, taking better account of covalency in the system, is needed to resolve the more subtle differences between coordinating triflate and EO oxygen atoms.

6. Conclusion

A number of clear observations can be made. The first is that there is no tendency for the Er^{3+} and $CF_3SO_3^-$ ions to aggregate in the PEO host at 300 K. Secondly, a variety of different coordination types appear in the simulation; these might well have been expected to contribute differently to the spectra. However, this is not apparent from the spectral calculations. Our inability to resolve contributions from different local environments may result from the high degree of covalency in the system. Extending the crystal-field model to take better account of covalency is thus essential; such models have been shown to work in well agreement with experimental data for other systems.[20]

The agreement between calculated and experimental absorption spectra is relatively good; the differences originate mainly in the free-ion parameters and the crystal-field model used. This result indicates that, using a more sophisticated crystal-field model, quantitative analysis of the different local coordination types occurring in amorphous rare-earth polymer materials can be possible with the presented technique.

Acknowledgements

This work has been supported by grants from The Swedish Natural Science Council (NFR) and from The Estonian Science Foundation Grant No. 4513.

References

1 *Rare-Earth-Doped Fiber Lasers and Amplifiers*, ed. M. Digonnet, Marcel Dekker, New York, 1993.
2 M. J. Weber, *The Role of Lanthanides in Optical Materials*, Lawrence Berkeley National Laboratory, University of California, Report LBL-37536, UC-404, 1995.
3 B. R. Judd, *Phys. Rev.*, 1962, **127**, 750.
4 G. S. Ofelt, *J. Chem. Phys.*, 1962, **37**, 511.
5 D. Brandell, M. Klintenberg, A. Aabloo and J. O. Thomas, *Int. J. Quantum Chem.*, 2000, **80**, 799.
6 A. Bernsson and J. Lindgren, *Solid State Ionics*, 1993, **60**, 31–36.
7 M. Furlani, A. Ferry, A. Franke, P. Jacobsson and B.-E. Mellander, *Solid State Ionics*, 1998, **129**, 113–155.
8 S. Neyertz, D. Brown and J. O. Thomas, *J. Chem. Phys.*, 1994, **101**(11), 10064.
9 G. Morrison, private communication.
10 A. K. Rappé, C. J. Casewitz, K. S. Colwell, W. A. Goddard and W. M. Skiff, *J. Am. Chem. Soc.*, 1992, **114**, 10024.
11 Jaguar, Schrodinger, Inc., Portland, OR.
12 The DL_POLY Project. W. Smith and T. Forester, TCS Division, Daresbury Laboratory, Daresbury, Warrington, UK WA4 4AD.
13 S. Edvardsson and M. Klintenberg, *J. Alloys Compd.*, 1998, **275**, 230.
14 K. Rajnak and B. G. Wybourne, *Phys. Rev.*, 1963, **132**, 280.
15 B. R. Judd, *Phys. Rev.*, 1966, **141**, 4.
16 M. Klintenberg, S. Edvardsson and J. O. Thomas, *J. Alloys Compd.*, 1998, **174**, 257–277.
17 M. Klintenberg, S. Edvardsson and J. O. Thomas, *Phys Rev. B: Condens. Matter*, 1997, **55**, 10369.
18 S. Edvardsson, M. Klintenberg and J. O. Thomas, *Phys. Rev. B: Condens. Matter*, 1996, **54**, 17476.
19 W. T. Carnall, P. R. Fields and R. Sarup, *J. Chem. Phys.*, 1972, **57**, 43.
20 Y. Shen and K. L. Bray, *Phys. Rev. B: Condens. Matter*, 1998, **58**, 5305.